

Standing on the Shoulder of a Giant: ISAAC, Antu, and Star Formation

M. McCAUGHREAN, H. ZINNECKER, M. ANDERSEN, G. MEEUS, and N. LODIEU

Astrophysikalisches Institut Potsdam

*If I have seen further, it is by standing on the shoulders of giants.
Isaac Newton, in a letter to Robert Hooke, 1676*

In the Beginning

Today's astronomers spend much of their time staring into regions where stars are forming, whether deep out in extragalactic space and far back in time, to watch as the first galaxies are assembled, or nearer to home, witnessing the fiery creation of new stars and planetary systems within our own Milky Way.

Crucial to these endeavours are the new 8–10-m diameter telescopic leviathans, equipped with powerful eyes sensitive to near-infrared light. For the high-redshift surveyors, the justification is straightforward: wavelengths grow as $(1+z)$ and surface brightness drops as $(1+z)^4$, making newly-born galaxies extremely faint, infrared sources. On the other hand, the nearest regions of ongoing star formation are “only” a few hundred parsecs away, yet the rationale is equally compelling. Stars are born from, and shrouded in, dense clouds of dust and molecular gas, out of whose obscuration visible light can barely escape. The same physics also yields substellar objects, the brown dwarfs, with masses perhaps as little as 1% of the Sun, feebly emitting their excess gravitational warmth as they cool and contract forever, never able to initiate nuclear hydrogen fusion. Young stars are encircled by disks of barely warm dust and gas, where swirling vortices gather mass to form planets, and the stars and disks conspire to generate immense supersonic jets of outflowing gas blasting out of the cocoon, lighting up great shocks glowing in the light of molecular hydrogen. Very often, all of this is going on at once, as stars are born in dense, crowded clusters, all interacting and competing with each other for survival.

All of which calls for the largest telescopes operated with sensitive infrared cameras and spectrographs. Wide field coverage is necessary to capture the whole story in a given region, but simultaneously with enough spatial resolution and dynamic range to disentangle the interactions between the many sources, and to ensure that we can detect even the faintest companions, disks, and planets immediately adjacent to their much brighter parents.

Fortunately, all of these demanding specifications are being well satisfied by the new large telescopes, optimized for infrared observing, equipped with state-of-the-art infrared array instruments, and situated on sites with excellent intrinsic atmospheric qualities.

In this article, we hope to illustrate the great qualitative and quantitative strides that star-formation studies have taken in the past few years, by looking at three highlights from our own work using the ESO Very Large Telescope UT1, Antu, and its facility near-infrared camera/spectrograph, ISAAC. In particular, we have chosen examples which illustrate a key theme running through our work, namely that of environmental impact, both in the effects that the birthplace of a star can have on its evolution, and in the back reaction that star formation can have on its surroundings. These are just a selection from the sample of young clusters and protostellar objects we are studying with the VLT (see also, e.g., Brandl et al. 1998; Zinnecker et al. 1999, 2002), and, of course, only a small subset of the work being carried out by the broad and active European star- and planet-formation community (Alves & McCaughrean 2002).

A momentary digression: the infrared Moore's law

We are by now all very familiar with the current generation of large telescopes, perhaps pre-eminent among which are the four 8.2-m diameter units of the VLT: this story could certainly not be told without them. However, photons must not only be collected but also detected, and an equally important issue in the present context is the huge parallel progress made in infrared detector technology over the 25 years or so since telescopes like the VLT were first proposed (Woltjer 1978).

At that time, the first purpose-built large infrared telescopes, such as the 3.8-m UKIRT on Mauna Kea, were about to go online, with instruments that focussed all of the primary mirror's light onto a single element detector. For much of the following decade, infrared astronomy continued in the same vein,

carrying out photometry or spectroscopy with single apertures, or laboriously mapping out extended regions one pixel at a time. Of course, many pioneering discoveries and advances were made, but the great sea change came in 1986, when infrared-sensitive detector arrays made their way out from behind the dark curtains of military secrecy and into open use on those large astronomical telescopes. With only 62×58 pixels, these arrays seem pitifully small in hindsight, and yet an instantaneous increase of almost 4,000 in the number of detectors in the focal plane of a telescope inspired the community and incited a true revolution.

It is a revolution that continues today. In the 1960s, Gordon Moore formulated his now-famous law that the number of transistors on semiconductor chips doubles every 12–24 months (Moore 1965): the same exponential growth in processor “power” has continued into the new millennium (Intel 2002). Interestingly, Alan Hoffman of Raytheon/SBRC has found that a similar scaling relation has tracked the introduction of progressively larger infrared detector arrays into common astronomical circulation, with a doubling of the number of pixels roughly every 18 months (see Fig. 1). Following SBRC's InSb 62×58 pixel arrays in 1986, the widespread adoption of the Rockwell NICMOS3 HgCdTe and SBRC InSb 256×256 pixel arrays occurred circa 1992, and that of the presently common generation of Rockwell HAWAII HgCdTe and SBRC Aladdin InSb 1024×1024 pixel arrays circa 1998. Indeed, ISAAC was commissioned in late 1998, and can switch between one or other of a HAWAII or Aladdin 1024×1024 pixel array.

So, while the VLT has “only” about five times the collecting area of UKIRT, ISAAC has a million times the number of pixels of any of UKIRT's first-generation instruments. This combined factor of five million improvement in the throughput (used in a deliberately loose sense here) available to infrared astronomers over just 20 years is quite dramatic, and has driven our understanding of star formation and early stellar evolution forward in leaps and bounds.

The Trapezium Cluster: towards a lower mass limit

It is well known that the entire life history of a star is almost uniquely determined by its mass, and yet it remains quite unclear how a star arrives at that mass in the first place. In a more general sense, we do not know how to predict the distribution of masses of a population of stars recently born from a molecular cloud, as found in a young cluster, for example, the so-called initial mass function (IMF).

In the broadest possible sense, the IMF has two important components: its form and its limits, that is, the shape of the IMF and where it cuts off at high and low mass. By measuring these parameters as a function of environment, including metallicity, cluster density, the presence of massive stars, for example, we can hope to place important constraints on any general theory of star formation that aims to predict the IMF and its variations. The single power-law form of the upper IMF in our galaxy has been known for many years (Salpeter 1955), but at lower masses, things become more interesting, with a turndown and peak in the IMF typically seen somewhere in the range $0.1\text{--}0.5 M_{\odot}$, that is, just above the stellar/substellar break (Kroupa 2001). While it seems self-evident that the processes of star formation know nothing about the nuclear fusion that later so brutally separates the fates of stars and brown dwarfs, the form of the IMF over this peak and down into the brown dwarf regime must nevertheless encode important physics. As a result, considerable effort has been invested in examining the substellar IMF in young clusters, searching for and investigating proto-brown dwarfs.

Most recently, several groups have been pursuing the IMF downwards in search of a possible lower cut-off. The theory of hierarchical fragmentation predicts that a collapsing molecular cloud will continue to break into ever smaller clumps as long they are able to radiate away their excess energy in less than the free-fall time for local collapse. However, opacity rises with density, and at some point the gas cannot cool quickly enough, becomes adiabatic and pressure-supported, and fragmentation ceases (Hoyle 1953). Traditionally, this lower cut-off is predicted to lie at $0.005\text{--}0.015 M_{\odot}$ or $5\text{--}15 M_{\text{Jup}}$ ($1 M_{\text{Jup}} = 0.001 M_{\odot}$) (Lynden-Bell & Low 1976; Rees 1976; Silk 1977), although more recent calculations suggest that it may be modified by the inclusion of magnetic fields, down to perhaps as little as $1 M_{\text{Jup}}$ (Boss 2001). More importantly, however, the whole fragmentation scenario down at low masses may have to be replaced by a more complex model involving a wide range of physical

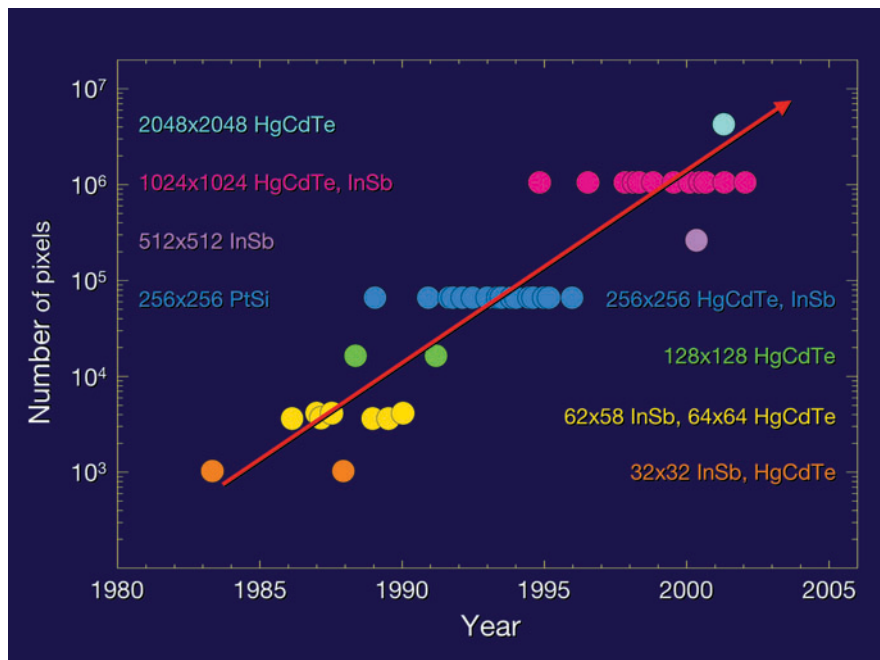


Figure 1: The growth of astronomical near-infrared array detectors, illustrated using a sample of 41 infrared cameras and plotting the year they were introduced into service against the number of pixels (rows \times columns) in their main detector. The dates have been randomised within the year of commissioning in order to provide a little horizontal separation. Some systems include more than one array, but typically with the same unit size: just the unit size is plotted for these. A wide range of telescope sizes is implicitly represented, from 1 to 10-m diameter, although there is no obvious tendency for the newest arrays to be introduced at either the smallest or largest telescopes. The red line represents Hoffman's version of Moore's Law, showing a doubling in pixel count roughly every 18 months over the past 20 years. Extrapolation points to 4096×4096 pixel arrays or mosaics (1.7×10^7 pixels) being the work-horse imaging systems by 2006.

processes, including supersonic turbulence (Padoan & Nordlund 2002), dynamical interactions between protostars (Bate, Bonnell, & Bromm 2002), and feedback due, for example, to strong bipolar outflows (Adams & Fatuzzo 1996) and ionizing radiation from massive stars (Palla & Stahler 2000). In addition, the existence of such objects with just a few Jupiter masses would be interesting in itself, as they could provide important insights into the very early evolution of giant planets, even if most astronomers would agree that free-floating objects formed directly from a molecular cloud core are not true planets like those formed in a circumstellar disk, and thus do not deserve that special name (cf. McCaughrean et al. 2001).

In any case, can we find such objects and any related mass cut-off directly, via observations? Although it might at first seem futile to think of searching for objects with just a few Jupiter masses at distances of a few hundred parsecs, they are remarkably warm and bright when young, and deep infrared imaging with large telescopes can now be used to go in search of them. One of the obvious targets for such a hunt is the Trapezium Cluster in Orion, probably the most populous and densest of the nearby young stellar clusters, with more than a thousand members crammed into its inner cubic parsec.

The cluster has proven an excellent site for probing the stellar initial mass function (Hillenbrand 1997), and is known to include many brown dwarfs (McCaughrean et al. 1995; Luhman et al. 2000; Hillenbrand & Carpenter 2000; Muench et al. 2001), and recent studies have suggested there may be sources down to as low as $\sim 10 M_{\text{Jup}}$ (Lucas & Roche 2000; Lucas et al. 2001). However, an even deeper wide-field survey was needed to test this finding and to search for any lower mass limit.

We have carried out such a survey using ISAAC over a 7×7 arcminute field centred on the well-known Trapezium OB stars, as shown in Figure 2, a true-colour J_s, H, K_s composite made from our initial data taken in 1999 (see McCaughrean et al. 2001). Adding data from 2000 and 2002, the final survey has 900 seconds integration time pixel per filter, and a mean seeing of 0.5 arcsec FWHM. These data go significantly deeper over a wide field than any previous infrared survey, with 3σ peak-pixel point source detection limits of $J_s, H,$ and K_s of $21^m.3, 20^m.0,$ and $19^m.6,$ respectively, limits ultimately set by the bright emission from the Orion Nebula. In the K_s band, these limits correspond roughly to $3 M_{\text{Jup}}$ at 450 pc, assuming an age of 1 Myr and a typical intracluster reddening of $A_V \sim 7^m$, using the DUSTY pre-main-sequence models of Chabrier et al. (2000).

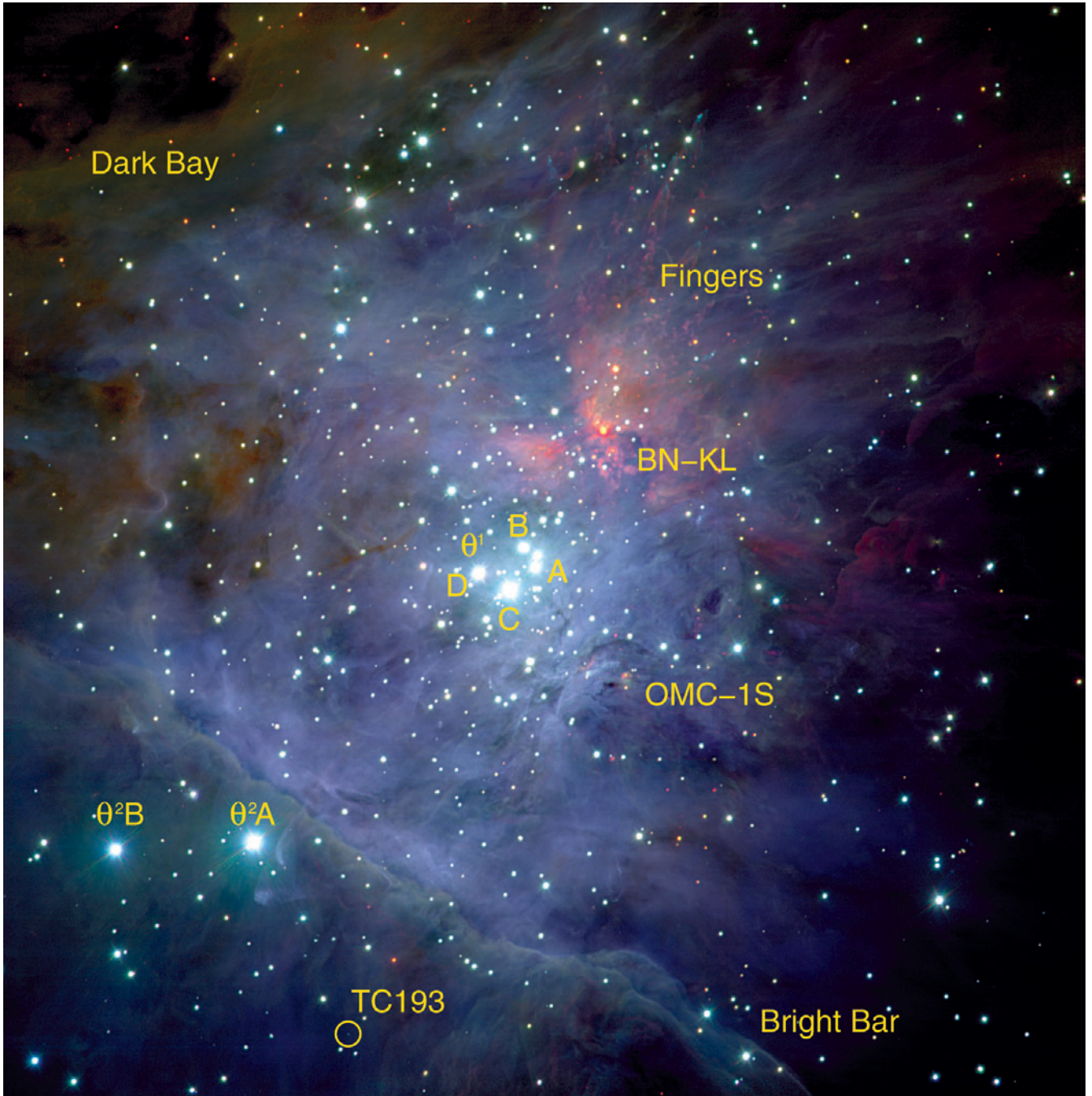


Figure 2: A true-colour near-infrared (1–2.5 μm) image of the Orion Nebula and Trapezium Cluster made using ISAAC on Antu in December 1999. The J_s data are shown as blue, H as green, and K_s as red. In this representation, cube root intensities and unsharp masking were used to compress the dynamic range and emphasise point sources, at a cost of some enhancement in the noise. The original version can be seen in McCaughrean et al. (2001). The image covers 7×7 arcmin, or 0.9×0.9 pc at the 450 pc distance to the nebula. North is up, east left. Total integration time in this subset of our data is 270 seconds per filter, and the seeing is 0.5 arcsec FWHM. For orientation, we have labelled the eponymous Trapezium OB stars at the centre of the image (θ^1 Ori A, B, C, & D); the two other well-known OB stars (θ^2 Ori A & B) just the south-east of the Bright Bar ionisation front; active star-formation centres embedded in the background molecular cloud, OMC-1S and BN-KL, the latter also being the origin of a massive outflow and the associated broad fan of shocked emission-line fingers to the north-west; and the Dark Bay, a region of high extinction in visible images that is penetrated here at infrared wavelengths. Also marked with a circle is TC193, a member of the Trapezium Cluster. With J_s , H , K_s magnitudes of 18^m4 , 17^m7 , and 17^m2 , respectively, this source is roughly 13 magnitudes fainter than θ^1 Ori C, illustrating the huge dynamic range that must be faced in such studies. TC193 is part of a sample for which we already have ISAAC spectroscopy: a preliminary estimate of its spectral type is L2, which would yield a mass of roughly $6 M_{\text{Jup}}$ assuming an age of 1 Myr, according to the models of Chabrier et al. (2000). Dereddening the near-infrared magnitudes back to the same isochrone would suggest a mass nearer $10 M_{\text{Jup}}$. Keep in mind also that it lies 2–3 magnitudes above our detection limits, and there are a significant number of potentially lower-mass sources to be studied in detail.

There are roughly 1200 sources in the survey region, 700 of which are fainter than the saturation limit of $K_s \sim 13^m$, and the ($J_s - H$) vs. H colour-magnitude diagram is shown in Figure 3. Without the aid of spectroscopy, it can

be notoriously difficult to convert a colour-magnitude diagram for a young, embedded cluster such as this into a mass function, and a discussion of the details and caveats of the methods used would fill an article in itself. To in-

vestigate how close we may get to our goal of finding a lower limit to the IMF, however, we can carry out a simple analysis. In Figure 3, we start by assuming that the cluster is 1 Myr old, taking a pre-main-sequence model iso-

chrone for that age and plotting it in the colour-magnitude diagram. The large and variable extinction in the cluster means a source must be individually dereddened back to that isochrone in order to determine its approximate mass, with care taken to ensure that a suitably complete extinction-limited sample is chosen before a mass function is derived. Next, we displace the 1 Myr isochrone by the median cluster reddening of $A_V \sim 7^m$, noting that the reddened $5 M_{\text{Jup}}$ point lies more or less at our observational completeness limit. Thus in principle, we can now derive an extinction-limited sample down to that $5 M_{\text{Jup}}$ limit. Finally, we divide the brown dwarf regime into just two equally-spaced logarithmic mass bins spanning the brown dwarf regime, from $5\text{--}20 M_{\text{Jup}}$ and from $20\text{--}80 M_{\text{Jup}}$. Between the unreddened and reddened isochrones, there are roughly 120 sources in the higher mass bin, compared to 30 in the lower bin. These numbers can be converted into a crude two-point mass function for brown dwarfs, with $dN/d \log M \propto M^{+1}$; this should be contrasted with the classical Salpeter mass function in the stellar domain which goes as $\propto M^{-1.35}$.

Thus, the mass function is falling steeply through the brown dwarf regime, a general result known previously for the Trapezium Cluster (see, e.g., McCaughrean et al. 1995; Hillenbrand & Carpenter 2000; Muench et al. 2002), but now extended all the way down well below the so-called deuterium-burning limit at $13 M_{\text{Jup}}$. Indeed, a more detailed analysis of the K_s data reveals that there are very few sources below $5 M_{\text{Jup}}$. Is this evidence for a lower mass cut-off? Such a claim would be premature: better mass determinations are required using spectroscopy to derive temperatures and surface gravities, and thus eliminate uncertainties due to differential reddening and non-coevality: we have begun this work using ISAAC, but much larger samples will be required. Second, a comprehensive comparison of the data against the wide range of available pre-main-sequence evolutionary and atmosphere models is required in order to test the robustness of the mass estimates. Third, it is clear that yet deeper imaging is required to probe well below the present limits, to ensure that we have delineated any such boundary on a statistically sound basis.

At first sight, this last point might appear trivial, since the present data only have 15 minutes integration time per filter. However, in practice, accumulating those 15 minutes was an onerous task. First multiply by three filters, then by nine on-source and four sky positions, a factor of two for detector readout, telescope offset, and standard star overheads, and a total of ~ 20 hours of clear conditions with excellent seeing were

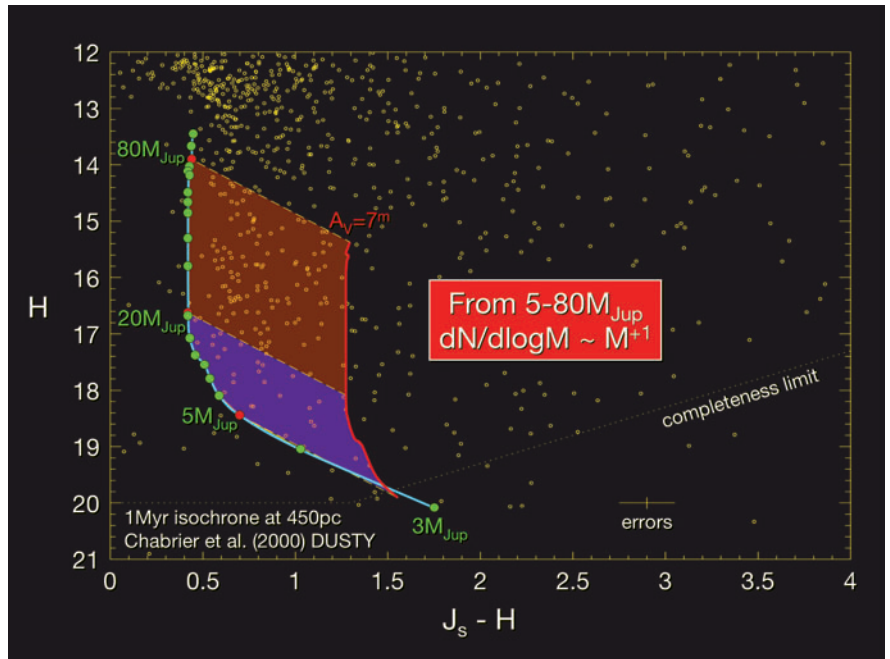


Figure 3: The (J_s-H) vs. H colour-magnitude diagram derived from our ISAAC imaging survey of the Trapezium Cluster (see Fig. 2). The completeness limit and typical photometric errors for sources just above this limit are shown. The 1 Myr isochrone from the pre-main sequence (DUSTY) models of Chabrier et al. (2000) is plotted assuming a distance of 450 pc. The great majority of the sources lie redwards of the isochrone due to intracluster dust extinction of up to $\sim 20^m$ and greater. There is a pile-up of sources at $H = 12^m\text{--}13^m$ due to the effects of deuterium burning, although sources brighter than this saturated within the 10 second on-chip integration time used for the survey. The number of potential brown dwarfs is large, but not dominant. As described in the text, we have also plotted the $0.005\text{--}0.08 M_{\odot}$ ($5\text{--}80 M_{\text{Jup}}$) segment of the isochrone reddened by $A_V \sim 7^m$: by counting sources in the $5\text{--}20$ and $20\text{--}80 M_{\text{Jup}}$ bins, we can see that the brown dwarf end of the IMF is clearly falling, as crudely characterised by the form $dN/d \log M \propto M^{+1}$.

needed. Also, as there are very bright stars in the field, the observations had to be made in visitor mode to avoid possible persistence effects impacting others in service mode. While trips to Paranal are always interesting, it unfortunately suffers relatively poor weather in peak Orion season, at the height of austral summer, and in the end, it has taken eight nights over three years to complete the survey to the present depth.

How much longer would be needed to get down from our current limit in the K_s band of $\sim 3 M_{\text{Jup}}$ to $1 M_{\text{Jup}}$, where, for example, the magnetically-mediated fragmentation limit may lie? Pre-main-sequence models can be used to assess this, although there are many uncertainties and differences between various models in this low-mass, low-temperature domain. For illustration, we use the well-known COND and DUSTY models of Isabelle Baraffe, Gilles Chabrier, France Allard, and collaborators, and in these models, a $1 M_{\text{Jup}}$ source at 1 Myr is predicted to be at least 2.8 magnitudes fainter than its $3 M_{\text{Jup}}$ counterpart in the K_s band. At least one infrared colour is required in order to provide a reddening estimate, and taking the H band, the most optimistic models predict that our $1 M_{\text{Jup}}$ source should again be 2.8 magnitudes fainter than the $3 M_{\text{Jup}}$

source. Thus even in the best case, we would require integration times roughly 175 times longer than we presently have, i.e., almost 44 hours on-source integration time per filter per field of view.

A wide field is necessary in order to obtain enough sources to ensure a statistically robust result, and using ISAAC to mosaic the cluster would obviously be prohibitive. A wide-field imaging system covering the whole cluster in one shot would improve matters greatly, but even then, once the two filters necessary plus sky and other overheads are accounted for, at least a month of clear observing nights on Orion would be required. Ultimately then, getting to the very bottom of this crucial question will require the NGST, as discussed briefly below.

The Eagle's EGGs: fertile or sterile?

At the opposite end of the mass spectrum from the sub- $10 M_{\text{Jup}}$ objects we have been searching for in the Trapezium Cluster, the eponymous OB stars at its heart pose a problem for their lower-mass neighbours. The massive stars yield a prodigious output of ultraviolet photons which not only sculpt and illuminate the Orion Nebula HII region, but also heat and ionise the

dense disks of dust and gas which surround the neighbouring young stars (O'Dell, Wen, & Hu 1993; Bally, O'Dell, & McCaughrean 2000). Are planetary systems able to form under this onslaught? As most stars form in clusters, this poses a major quandary in our attempts to understand the birth statistics of the galactic planetary population. However, massive stars can have an impact even earlier in the star formation process. When they first ignite, their ionising photons and strong winds collide with any nearby molecular cloud material, first compressing dense cores and then ripping them apart. Can new stars form via radiative implosion before the cores are destroyed (Larosa 1983; Bertoldi 1989; Lefloch & Lazareff 1994)? How are the properties of any pre-existing protostars affected by having their parental cores blown away before accretion has ended?

A case in point is M 16, the Eagle Nebula, where the famous HST images of Hester et al. (1996) delineated in exquisite detail three so-called elephant trunks, parsec-long columns of gas and dust being ionised by OB stars of the adjacent NGC 6611 cluster. Around the fringes of the trunks, Hester et al. resolved a population of small, dense knots, which they named EGGs for evaporating gaseous globules. As strictly correct as the acronym may have been, it also encapsulated a less obvious proposition, namely that the EGGs are also eggs, the birthplaces of new stars. Based on a couple of plausible associations between EGGs and stars, Hester et al. hypothesised that the full population of 73 EGGs identified in their images might harbour a plethora of young stars about to be exposed by the ionizing flux of the OB stars, thus terminating accretion and helping to define their final masses. Indeed, Hester et al. went further, and suggested that if most stars form in such an environment, perhaps the form of the IMF is determined by the impact of OB stars.

This far-reaching hypothesis needed testing. The optical HST images were unable to probe the interiors of most of the dense EGGs, to assess how many of them truly contained young stars, and deep infrared observations are called for in order to penetrate the extinction and make a detailed census. In addition, these observations must be at high spatial resolution, as the median EGG diameter is just 1000 AU or 0.5 arcsec at 2 kpc, and have to span a wide field of view, in order to cover the whole elephant-trunk system and make a detailed statistical study of contamination by the dense field star population seen towards and beyond M 16. Early attempts either had inadequate resolution (McCaughrean 1997) or too limited a field (Currie et al. 1997), and

only the combination of the VLT, ISAAC, and service mode observations was able to deliver the deep, wide-field images with superb seeing necessary to carry out the definitive survey of this astronomical icon. Our data were obtained in 2001, covering a wide field (10×10 arcmin) with excellent seeing-limited resolution (0.35 arcsec FWHM), yielding 3σ peak pixel point source detections at J_s , H , and K_s of $22^m.6$, $21^m.3$, and $20^m.4$, respectively. Assuming an age of 1 Myr, these limits correspond to the detection of a $0.08 M_\odot$ source embedded in 30^m of visual extinction, and even brown dwarfs should be visible through less extinction (McCaughrean & Andersen 2002).

The resulting colour composite image covering just the elephant trunks is shown in Figure 4: the full field of view can be seen in McCaughrean & Andersen (2001). A detailed examination of the 73 EGGs shows that just 11 appear to harbour infrared sources, as marked in Figure 4. Four of these appear to be low-mass stars, while the other seven may be brown dwarfs, several of which cluster near the tip of the largest elephant trunk, close to a massive ($4\text{--}10 M_\odot$) young protostar (YSO1; see also Sugitani et al. 2002; Thompson, Smith, & Hester 2002). Although selection effects and uncertainties abound, there does indeed appear to be some limited star formation going on in the elephant trunks. However, a major question remains completely unanswered. Did these objects already exist in the trunks, only to be revealed now by the passage of the NGC 6611 ionisation front, or was their formation indeed initiated by that front triggering the radiative implosion of dense cores? If the former model holds, then we might expect to find a distribution of young stars and brown dwarfs embedded within the densest parts of the trunks, not just at the ionised periphery: due to the extinction however, this is also an experiment which will probably have to await a combined thermal-infrared and millimetre survey by the NGST and ALMA, respectively.

And finally, we must be careful not to develop tunnel vision, mistaking the single HST WFPC-2 field of view version of M 16 for a detached, isolated object, as the makers of the film version of Carl Sagan's "Cosmos" did in their otherwise bravura opening sequence. The real action in the region appears to have taken place in NGC 6611, where a cluster of thousands of stars has formed within the past few million years, apparently with a rather normal IMF (Hillenbrand et al. 1993). The ongoing destruction of the adjacent elephant trunks and the limited star formation taking place within them may ultimately prove to be a sideshow in the grander scheme of things, albeit a beautiful one.

HH212: the prototypical protostellar jet

In M 16, we have seen the impact massive stars can have on their environment. However, even low-mass stars can play an important part in the feedback loop, as we see in our last example, an enigmatic protostellar source near Orion's belt. In the mid-1980s, one of us (HZ) had become interested in very young binary systems, very few of which were known at the time. A newly-discovered cold, dense molecular cloud core, however, IRAS 05413-0104, appeared to be an ideal target in which to go looking for a low-mass protobinary system. The opportunity came in 1987, during the commissioning of the original IRCAM on UKIRT. With only a 62×58 pixel array, there was an inevitable trade-off in IRCAM between field of view and spatial resolution, the former generally favoured over the latter. This was in part because of the lure of finally being able to map large regions, in part because the typical seeing at UKIRT was not thought to be that great, and in part because the received wisdom from single-element detectors was that small, noisy pixels would make it impossible to detect low-surface-brightness emission, forgetting however that one only had to integrate long enough to become background limited. In any case, the IRCAM field of view in its 0.6 arcsec/pixel mode was just 37×35 arcsec, and in retrospect, these parameters conspired to lead us completely astray for several years. A single K-band image was taken, revealing two, apparently point sources separated by 7 arcsec. Without further ado, we took this to confirm all of our expectations and preconceptions, and as a consequence, IRAS 05413-0104 was written up as a young binary system (Zinnecker 1989; Zinnecker et al. 1992).

Everything changed a few years later during an observing run at the 3-m IRTF on Mauna Kea. While defining macros to observe one target, a brief opening in the proceedings made it possible to slew to IRAS 05413-0104 for follow-up imaging using the facility camera, NSFCAM. With its 256×256 pixel array, NSFCAM had improved sampling and field compared to IRCAM, 0.3 arcsec/pixel and 77×77 arcsec, respectively. As soon as the first image arrived, it was clear this was something other than a simple binary system: the original two sources were now seen to be extended, not point-like, and they appeared to be just the innermost pair of a long, linear trail of faint nebular knots. Guessing that this was in fact a young jet, not a protobinary, we switched to a narrow-band filter at $2.12 \mu\text{m}$ designed to trace emission from hot molecular hydrogen and after some mosaicing, a spectacular large outflow was revealed, later to be named HH



Figure 4: A true-colour near-infrared ($1\text{--}2.5\ \mu\text{m}$) image of the well-known elephant trunks (or columns, C1, C2, C3) in M 16, the Eagle Nebula, made with data taken with ISAAC on Antu in April–May 2001. The J_s data are shown as blue, H as green, and K_s as red. The cube root of the intensities was taken to compress the dynamic range before normalizing and combining the three mosaics. The main image covers 2.6×3.6 arcmin or 1.5×2.0 pc assuming a distance of 1.9 kpc to M 16, and is a subsection of the full 9×9 arcmin data set that can be seen in McCaughrean & Andersen (2001). North is up, east left. Total integration time is 1200 seconds in J_s , and 300 seconds in each of H and K_s . The seeing is 0.35 arcsec FWHM. The small subimages have been magnified by a factor of 2.9 and each covers 18.5×18.5 arcsec (0.17×0.17 pc). Labels mark evaporating gaseous globules (EGGs) identified in the optical HST data of Hester et al. (1996) which we find to be associated with low-mass stars and brown dwarfs as described in the text. Also shown are E23, an EGG with no near-infrared point source, but thought to contain an embedded protostar driving a collimated jet; YSO1 and YSO2, massive sources in the tips of C1 and C2, respectively; and HH 216, an optically-visible Herbig-Haro object (Andersen et al. 2002). Due to the large dynamic range, some of the very faintest sources are not easily seen in the subimages, but can be seen in the original data. From McCaughrean & Andersen (2002).

212, not at all coincidentally after the wavelength at which it was emitting. Subsequent deeper observations a year later using the 256×256 pixel MAGIC camera on the Calar Alto 3.5-m telescope fully delineated the extreme bipolar symmetry of the flow, with a series of compact knots and bowshocks equidistantly spaced on either side of the centre. It is highly unlikely that inhomogeneities in the surrounding ambient medium would give rise to such symmetry. Rather, the symmetric sequence of features appears to represent a ticker-tape record of the accretion history of the very young central protostars, with variations in the infall onto the protostar being reflected in sequences of knots and bowshocks in the corresponding outflow (Zinnecker, McCaughrean, & Rayner 1998).

However, the unknown parameter in this chart recorder is how quickly the paper is moving, i.e., the timescales involved. How often are new knots emitted? How fast are they moving when emitted? How do they decelerate when they interact with the ambient medium? What is their time-averaged impact on the surrounding medium? High-resolution spectroscopy of the two inner knots in the $2.12\text{-}\mu\text{m}$ line shows almost identical radial velocities, indicating that the jet must lie very close to the plane of the sky (Zinnecker et al. 1998), and thus proper motion measurements are required to reveal the velocity structure of the jet. Typical peak outflow speeds measured in young jets are of the order of $100\text{--}200\text{ km s}^{-1}$, equivalent to just $0.05\text{--}0.1\text{ arcsec/yr}$ at 400 pc. But while two images separated by 10 years might appear to be sufficient, it is important to measure the motions as rapidly as possible, as shocked molecular hydrogen cools on timescales of 1–2 years, and thus over longer timescales, there is no guarantee that it is the same packet of gas that is glowing. In addition, it is important to measure lower velocities where the outflowing jet decelerates into the surrounding gas.

Thus we require deep, high spatial resolution imaging separated by reasonably short intervals. We are observing HH 212 in the $2.12\text{-}\mu\text{m}$ line with ISAAC once per year over a five-year period. Service mode observing almost guarantees that we will obtain the desired excellent seeing ($< 0.4\text{ arcsec}$) for the annual two hours of integration time, and the relatively large ISAAC field means that only a two-position mosaic is required to cover the whole jet, which in turn ensures reasonably accurate proper-motion determinations. Adaptive optics imaging is not an option in this region given the lack of a suitably bright guide star, and distortion problems introduced by AO over wide fields might also be a concern. To date, we have imaged the jet three times over a 16-month period, and are al-

ready able to identify velocities in the inner knots of $100\text{--}200\text{ km s}^{-1}$, although the observations must be continued in order to extend the sensitivity down to 20 km s^{-1} or so, where the outer bow shocks sweep up the ambient medium.

In the meantime, however, we have combined the extant data to make a single extremely deep image as shown in Figure 5, which has a total integration time of 282 minutes in the central half, and 141 minutes in the outer parts. This is by far the deepest infrared image obtained of a young protostellar jet, with 4.7 hours on an 8.2-m telescope to be compared to the typical longest observations of any other system of 30 minutes on a 4-m-class telescope. In addition, the coadded spatial resolution is an excellent 0.34 arcsec FWHM , with one data set having $0.2\text{--}0.25\text{ arcsec}$ resolution over its full two hour span, equal to the diffraction-limited spatial resolution of the HST at the same wavelength. Finally, even though the jet is indeed seen to move over the 16-month baseline, the maximum shifts are on the order of a single ISAAC pixel (0.148 arcsec), and thus any blurring introduced is invisible at the scale shown here.

While the basic symmetry of the jet is obviously maintained, the greatly improved sensitivity and resolution reveal important new details. The innermost knots are all resolved into bowshocks, small counterparts to the larger bows further out, and overall, the flow appears very similar to simulations made of so-called “hammer jets” (Suttner et al. 1997; Volker et al. 1999), where a time-variable jet sends out a series of pulses of dense gas leading to small bowshocks: these subsequently merge into a larger bowshock plowing its way through the ambient medium. However, the image reveals almost continuous emission between the knots following apparently sinuous channels, and the origin of this emission is not entirely clear: why are there continuous shocks between the bows?

Near the base of the jet, there is a pair of diffuse nebulae that broadly resemble the parabolic reflection nebulae associated with circumstellar disks around young stellar objects, as seen in HH 30, IRAS 04302+2247, and Orion 114–426 (McCaughrean, Stapelfeldt, & Close 2000). However, the HH 212 nebulae are separated by roughly 5.5 arcsec or 2200 AU , and comparison with continuum data shows that these nebulae are in fact emitting almost exclusively in the $2.12\text{-}\mu\text{m}$ line, which apparently rules out the central YSO as the source of illumination. Finally, the deep data show that these nebulae extend up and along the jet. It seems likely that the two brightest, innermost knots of the jet are acting as huge spotlights hanging in space, their light being

reflected off the uppermost surfaces of the large flattened, rotating molecular cloud core associated with the central protostar (Lee et al. 2000; Wiseman et al. 2001), as well as the inner edges of the cavity being excavated by the outflow in the larger parent core. Alternatively, it may be that gas along the edge of the cavity is being lightly shocked and that the emission is *in situ*, not reflected.

Finally, close inspection of the VLT image reveals that a substantial fraction of the sources in the surrounding field are in fact background galaxies, confirming that the parent core is very compact and quite detached from the nearby Orion B molecular cloud complex. This is especially evident at the north-east end, where the outer bowshock appears to pass close to a cluster of galaxies, and begs the question of how there can be any ambient medium in the region to be shocked. Conversely, in one of the largest departures from symmetry, there is an additional large bowshock at the south-west end, probably formed as the jet prow into another cloud core, as signposted by the presence of a bright source surrounded by nebulosity and an apparently edge-on disk system. This interaction between one low-mass protostar and a dense core apparently containing another reminds us again that the cumulative effects of feedback cannot be neglected when trying to understand the formation of a population of young stars, whether they be in a dense cluster or more distributed over a larger molecular cloud.

A look to the near future

The first few years of VLT operation have been a great success, and ISAAC has been an outstanding workhorse instrument, as hopefully witnessed by the data shown in this article and elsewhere. However, there is a fly in the ointment: all of the projects described in this article relied on mosaicing to cover the desired field, which is not only inefficient, but also compromises accuracy when it comes to PSF-fitting photometry, proper-motion monitoring, and detection of very extended low-surface-brightness emission. As a result, it is worth taking a brief look at the future of wide-field near-infrared imaging at ESO, and thus by extension, how our studies may be further improved.

The standard answer is VISTA, the 4-m survey telescope which will feed a huge infrared camera covering the equivalent of $42 \times 42\text{ arcmin}$ at 0.31 arcsec/pixel with $16\,2048 \times 2048$ pixel arrays. It is argued that VISTA eliminates the need for a wide-field camera on the VLT, since for large-area surveys, it will make up with field of view what it lacks in collecting area. But there are caveats. First, the VISTA camera

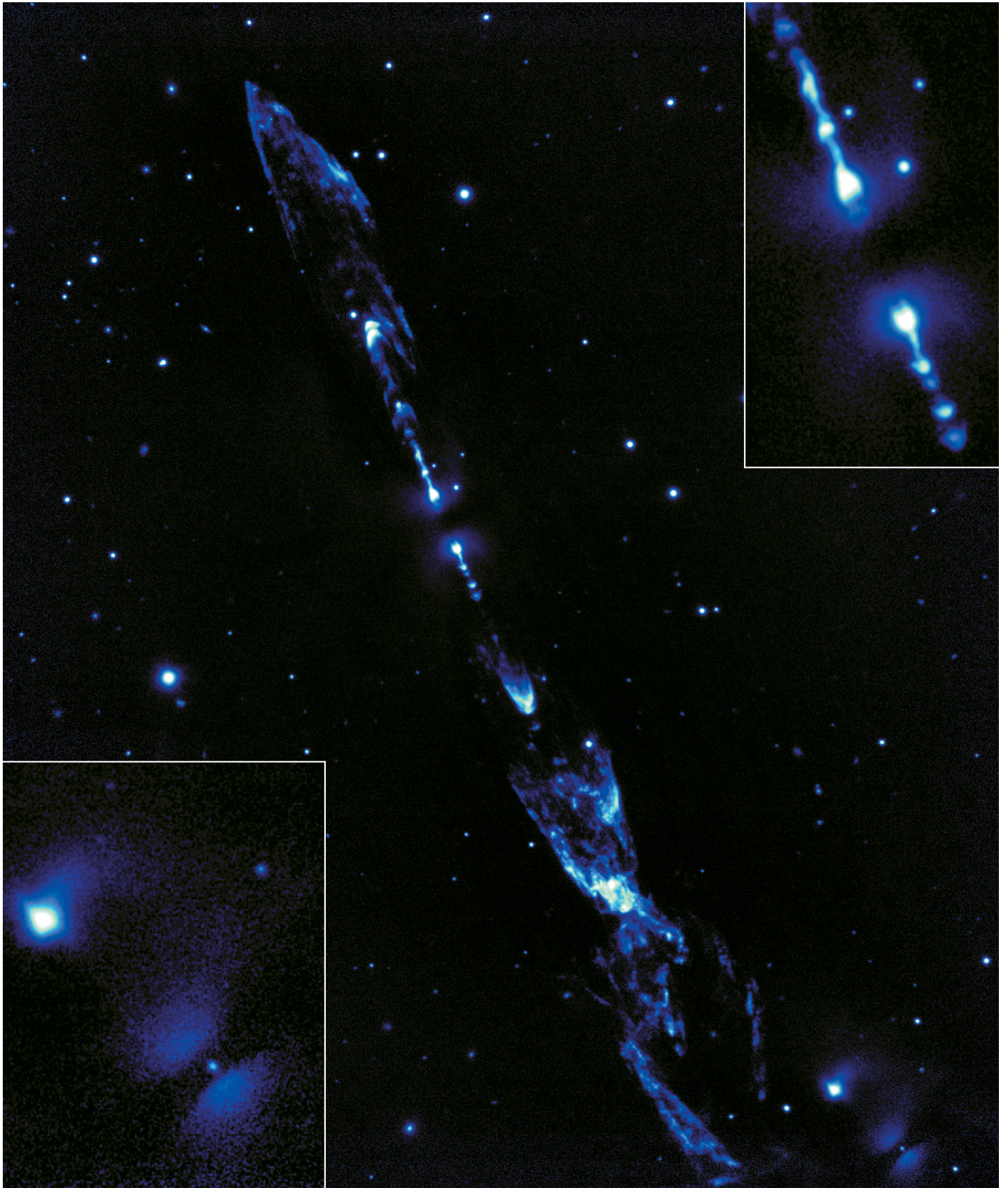


Figure 5: A deep image of the protostellar jet, HH212, in the $2.122\ \mu\text{m}\ \nu = 1-0\ S(1)$ line of molecular hydrogen, made using ISAAC on Antu, with data from October 2000, October 2001, and January 2002. North is up, east left. Total integration time in the central half is 282 minutes, yielding a 3σ per pixel limiting surface brightness sensitivity there of $1.2 \times 10^{-19}\ \text{W m}^{-2}\ \text{arcsec}^{-2}$. The image covers $3.2 \times 3.9\ \text{arcmin}$ or $0.37 \times 0.45\ \text{pc}$ assuming a distance of 400 pc to HH212. The resolution is seeing limited at $0.34\ \text{arcsec}$ FWHM. Intensities have been scaled logarithmically. Continuum emission has not been subtracted as the jet is known to be emitting almost exclusively in the S(1) line: however, continuum sources such as field stars and galaxies remain visible. As discussed in the text, the nebulosity surrounding the base of HH212 is line emission, while the bipolar nebula at the south-west end of the image is seen in continuum emission, and is most likely a large circumstellar disk. Judging from broad-band data, the point source at the centre of the southwest nebula appears to be an unrelated field star. The two subimages in the corners have been expanded by a factor of 2.5, and show the south-west bipolar nebula (lower left) and the inner knots of HH 212 (upper right) in more detail. From McCaughrean et al., in preparation.

will not have the contiguous field which is often so important for star-formation targets: mosaicing will still be required. Second, for observations of a single field trying to reach a given faint flux limit, the VLT will be four times quicker than VISTA. Third, the infrared seeing is frequently excellent on the VLT, and the VISTA image scale will not take proper advantage of it: a camera with an image scale similar to ISAAC's would make it quicker yet for point sources, as well as yielding superior resolving power for extended sources, and reducing confusion in crowded fields.

On the VLT itself, NAOS/CONICA delivers excellent spatial resolution, but over a smaller field than even ISAAC. NIRMOS should include an imaging mode covering roughly 16×14 arcmin at 0.2 arcsec/pixel, but again not contiguous, and only covering 1–1.8 μm , making it of limited utility for studies of low-mass or deeply embedded, cool sources, or shocked H_2 emission associated with outflows. Among the VLT second-generation instruments under consideration, there is a near-infrared multiobject spectrograph, KMOS, which would extend to 2.5 μm , but which may or may not include an imaging mode. In any event, according to present planning, it does not appear that any wide-field imager covering the whole 1–2.5 μm region would be in operation on Paranal before 2007.

Hoffman's version of Moore's law suggests that we should have already had a 2048×2048 pixel infrared array camera available in 2001, and indeed, Gemini-South commissioned such a camera (FLAMINGOS) at that time. In the 2004–2006 timeframe, 4096×4096 pixel cameras should be shouldering most of the load, and indeed, several ESO member states are developing such cameras for their 4-m-class telescopes, including WFCAM for UKIRT and WIRCAM for the CFHT. Thus it seems reasonable to explore the options for developing a wide-field imager for the VLT. A straightforward direct imager with a 2×2 mosaic of 2048×2048 pixel arrays would cover a 10×10 arcmin field at the same 0.15 arcsec/pixel scale as ISAAC, sampling the kind of excellent infrared seeing seen in this article, and would be very well suited to deep pointed imaging of embedded star clusters, and outflows, as well as nearby galaxies and distant galaxy clusters.

Looking even further ahead, the joint NASA/ESA/CSA Next Generation Space Telescope will combine a large primary mirror (in this case, 6.5 m in diameter), with diffraction-limited resolution (0.08 arcsec at 2 μm) over a field of more than 3×3 arcmin, and a location at the Sun-Earth L2 point where passive cooling to 50 K will avoid the scourge of OH airglow and thermal background fought from the ground.

Together, these features will yield extraordinary gains in sensitivity from 0.6 to 28 μm for both imaging and spectroscopy. As examples in the context of this article, consider a survey for point sources at 2 μm : the NGST should go more than 6 magnitudes deeper than ISAAC in the same integration time, and folding in all factors, the NGST will be roughly 10^4 times faster than a present-day 8-m telescope, completing in just one hour what would take literally years of ground-based observing time.

Thus, when the NGST is launched in 2010, we will take yet another giant leap in the ongoing revolution that is infrared astronomy, less than 25 years after the first infrared arrays were brought to UKIRT and 12 years after the opening of the VLT. In tandem with the wide-field, high spatial resolution millimetre and submillimetre imaging to be enabled by ALMA in the same timeframe, the future for star-formation studies looks very rosy indeed. Given what we have seen in the past decade, who knows what surprises lie ahead?

Acknowledgements

It is a great pleasure to thank our many friends at ESO, on Paranal and in Garching, especially those who built ISAAC, those who look after it, those who ensure it works well with the VLT, and those who have helped us get the very best data out of it in both visitor and service mode. In alphabetical order, these include Fernando Comerón, Jean-Gabriel Cuby, Vanessa Doublier, Gerd Finger, Roberto Gilmozzi, Olivier Hainaut, Bruno Leibundgut, Chris Lidman, Gianni Marconi, Alan Moorwood, Almudena Prieto, Dave Silva, and Jason Spyromilio. MJM would like to thank Isabelle Baraffe, Michael Meyer, and Francesco Palla for useful input, and the Institute of Astronomy in Cambridge, where much of this paper was written, for their hospitality. This work was funded in part by the EC Research Training Network "The Formation and Evolution of Young Stellar Clusters" (HPRN-CT-2000-00155) and DLR grants 50-OR-0004/9912.

References

- Adams, F.C. & Fatuzzo, M. 1996, *ApJ*, **464**, 256.
 Alves, J. & McCaughrean, M.J. 2002, eds. *The Origins of Stars and Planets: The VLT View* (Berlin: Springer Verlag).
 Andersen, M., Reipurth, B., Knude, J. et al. 2002, *A&A*, in press.
 Bally, J., O'Dell, C.R., & McCaughrean, M.J. 2000, *AJ*, **119**, 2919.
 Bate, M.R., Bonnell, I., & Bromm, V. 2002, *MNRAS*, **332**, L65.
 Bertoldi, F. 1989, *ApJ*, **346**, 735.
 Boss, A.P. 2001, *ApJ*, **551**, L167.
 Brandl, B., Brandner, W., Eisenhauer, F., Moffat, A.F.J., Palla, F., & Zinnecker, H. 1999, *A&A*, **352**, L69.
 Chabrier, G., Baraffe, I., Allard, F., & Hauschildt, P. 2000, *ApJ*, **542**, 464.

- Currie, D., Kissell, K., Shaya, E. et al. 1996, *The Messenger*, **86**, 31.
 Hester, J.J., Scowen, P.A., Sankrit, R. et al. 1996, *AJ*, **111**, 2349.
 Hillenbrand, L.A. 1997, *AJ*, **113**, 1733.
 Hillenbrand, L.A. & Carpenter, J.M. 2000, *ApJ*, **540**, 236.
 Hillenbrand, L.A., Massey, P., Strom, S.E., & Merrill, K.M. 1993, *AJ*, **106**, 1906.
 Hoyle, F. 1953, *ApJ*, **118**, 513.
 Intel 2002, <http://www.intel.com/research/silicon/mooreslaw.htm>
 Larosa, T.N. 1983, *ApJ*, **274**, 815.
 Lee, C.-F., Mundy, L.G., Reipurth, B., Ostriker, E.C., & Stone, J.M. 2000, *ApJ*, **542**, 925.
 Lefloch, B. & Lazareff, B. 1994, *A&A*, **289**, 559.
 Lucas, P.W. & Roche, P.F. 2000, *MNRAS*, **314**, 858.
 Lucas, P.W., Roche, P.F., Allard, F., & Hauschildt, P. 2001, *MNRAS*, **326**, 695.
 Luhman, K.L., Rieke, G.H., Young, E.T. et al. 2000, *ApJ*, **540**, 1016.
 Low, C. & Lynden-Bell, D. 1976, *MNRAS*, **176**, 367.
 McCaughrean, M.J. 1997, in *Herbig-Haro Flows and the Birth of Low Mass Stars*, eds. B. Reipurth & C. Bertout, IAU Symp. 182, 551.
 McCaughrean, M.J., Alves, J., Zinnecker, H., & Palla, F. 2001, ESO press release (<http://www.eso.org/outreach/press-rel/pr-2001/phot-03-01.html>).
 McCaughrean, M.J. & Andersen, M. 2001, ESO press release (<http://www.eso.org/outreach/press-rel/pr-2001/phot-37-01.html>)
 McCaughrean, M.J. & Andersen, M. 2002, *A&A*, **389**, 513.
 McCaughrean, M.J., Reid, I.N., Tinney, C.G. et al., 2001, *Science* (Letters), **291**, 1487.
 McCaughrean, M.J., Stapelfeldt, K.R. & Close, L.M. 2000, in *Protostars & Planets IV*, eds. V. Mannings, A.P. Boss, & S.S. Russell (Tucson: Univ. Arizona Press), p. 485.
 McCaughrean, M.J., Zinnecker, H., Rayner, J.T., & Stauffer, J.R. 1995, in *The Bottom of the Main Sequence and Beyond*, ed. C.G. Tinney, (Berlin: Springer Verlag), p. 209.
 Moore, G.E. 1965, *Electronics*, **38**, 8.
 Muench, A.A., Lada, E.A., Lada, C.J., & Alves, J. 2002, *ApJ*, **573**, 366.
 O'Dell, C.R., Wen, Z., & Hu, X. 1993, *ApJ*, **410**, 696.
 Padoan, P. & Nordlund, Å. 2002, *ApJ*, submitted (astro-ph/0205019).
 Palla, F. & Stahler, S.W. 2000, *ApJ*, **540**, 255.
 Rees, M.J. 1976, *MNRAS*, **176**, 483.
 Salpeter, E.P. 1955, *ApJ*, **121**, 161.
 Silk, J. 1977, *ApJ*, **214**, 152.
 Sugitani, K., Tamura, M., Nakajima, Y. et al. 2002, *ApJ*, **565**, L25.
 Suttner, G., Smith, M.D., Yorke, H.W., & Zinnecker, H. 1997, *A&A*, **318**, 595.
 Thompson, R.I., Smith, B.A., & Hester, J.J. 2002, *ApJ*, **570**, 749.
 Völker, R., Smith, M.D., Suttner, G., & Yorke, H.W. 1999, *A&A*, **343**, 953.
 Wiseman, J., Wootten, A., Zinnecker, H., & McCaughrean, M.J. 2001, *ApJ*, **550**, L87.
 Woltjer, L. 1978, in *Optical Telescopes of the Future*, eds. F. Pacini, W. Richter, & R.N. Wilson (Geneva: ESO), p. 5.
 Zinnecker, H. 1989, in *Low Mass Star Formation and Pre-main Sequence Objects*, ed. B. Reipurth, (Garching: ESO), p. 447.
 Zinnecker, H., Andersen, M., Brandl, B. et al. 2002, in *Extragalactic Star Formation*, eds. E. Grebel, D. Geisler, & D. Minniti, IAU Symposium 207, in press.
 Zinnecker, H., Bastien, P., Acoragi, J.-P., & Yorke, H.W. 1992, *A&A*, **265**, 726.
 Zinnecker, H., Krabbe, A., McCaughrean, M.J. et al. 1999, *A&A*, **352**, L73.
 Zinnecker, H., McCaughrean, M.J., & Rayner, J.T. 1998, *Nature*, **394**, 862.